

# $\alpha$ -Synuclein Expression in Rat Substantia Nigra Suppresses Phospholipase D2 Toxicity and Nigral Neurodegeneration

Oleg S Gorbatyuk<sup>1-4</sup>, Shoudong Li<sup>1,2,4</sup>, Frederic Nha Nguyen<sup>2,3,5</sup>, Fredric P Manfredsson<sup>2,3,5</sup>, Galina Kondrikova<sup>1,2,4</sup>, Layla F Sullivan<sup>1-5</sup>, Craig Meyers<sup>1,2,4</sup>, Weijun Chen<sup>1,2,4</sup>, Ronald J Mandel<sup>2,3,5</sup> and Nicholas Muzyczka<sup>1-4</sup>

<sup>1</sup>Department of Molecular Genetics and Microbiology, College of Medicine, University of Florida, Gainesville, Florida, USA; <sup>2</sup>The Powell Gene Therapy Center, College of Medicine, University of Florida, Gainesville, Florida, USA; <sup>3</sup>McKnight Brain Institute, University of Florida, Gainesville, Florida, USA; <sup>4</sup>UF Genetics Institute, University of Florida, Gainesville, Florida, USA; <sup>5</sup>Department of Neuroscience, College of Medicine, University of Florida, Gainesville, Florida, USA

We present genetic evidence that an *in vivo* role of  $\alpha$ -synuclein ( $\alpha$ -syn) is to inhibit phospholipase D2 (PLD2), an enzyme that is believed to participate in vesicle trafficking, membrane signaling, and both endo- and exocytosis. Overexpression of PLD2 in rat substantia nigra pars compacta (SNc) caused severe neurodegeneration of dopamine (DA) neurons, loss of striatal DA, and an associated ipsilateral amphetamine-induced rotational asymmetry. Coexpression of human wild type  $\alpha$ -syn suppressed PLD2 neurodegeneration, DA loss, and amphetamine-induced rotational asymmetry. However, an  $\alpha$ -syn mutant defective for inhibition of PLD2 *in vitro* also failed to inhibit PLD toxicity *in vivo*. Further, reduction of PLD2 activity in SNc, either by siRNA knockdown of PLD2 or overexpression of  $\alpha$ -syn, both produced an unusual contralateral amphetamine-induced rotational asymmetry, opposite to that seen with overexpression of PLD2, suggesting that PLD2 and  $\alpha$ -syn were both involved in DA release or reuptake. Finally,  $\alpha$ -syn coimmunoprecipitated with PLD2 from extracts prepared from striatal tissues. Taken together, our data demonstrate that  $\alpha$ -syn is an inhibitor of PLD2 *in vivo*, and confirm earlier reports that  $\alpha$ -syn inhibits PLD2 *in vitro*. Our data also demonstrate that it is possible to use viral-mediated gene transfer to study gene interactions *in vivo*.

Received 5 February 2010; accepted 5 June 2010; published online 27 July 2010. doi:10.1038/mt.2010.137

## INTRODUCTION

$\alpha$ -synuclein ( $\alpha$ -syn) is a 140 amino acid protein that is present in neurons at both cytoplasmic location and in membranes. Mutations in  $\alpha$ -syn, as well as overproduction of  $\alpha$ -syn, can cause

early onset Parkinson's disease in humans and loss of dopamine (DA) neurons in rodent and primate animal models.<sup>1</sup> To date, the biological function of  $\alpha$ -syn remains unclear.

One of the possible functions of  $\alpha$ -syn is the inhibition of phospholipase D (PLD).<sup>2</sup> Two major forms of PLD have been identified, PLD1 and PLD2, as well as some splice isoforms.<sup>3</sup> PLD cleaves phosphatidylcholine to produce phosphatidic acid (PA) and free choline. Phosphatidylinositol 4,5 bisphosphate is an essential cofactor for the reaction; thus, like  $\alpha$ -syn, PLDs interact with membranes. More important,  $\alpha$ -syn was identified as a potent inhibitor of PLD2 (ref. 2) in bovine and mouse brain extracts. Later, inhibition was also demonstrated for PLD1 (ref. 4). Mutational analysis of  $\alpha$ -syn revealed that substitution of ser129 with an acidic residue creates a mutant that is less toxic than wild type *in vivo*,<sup>5,6</sup> and is defective as an inhibitor of PLD2 *in vitro*.<sup>7</sup>

Based on cell culture and *in vitro* experiments, essentially three major types of functions have been demonstrated for PLD2. First, the product of PLD2 (PA) is a signaling molecule involved in pathways that control a wide variety of cellular processes, including cell proliferation via Raf and cell survival via TOR.<sup>8</sup> PLD2 production of PA is often coupled locally with phosphatidylinositol-4-phosphate 5 kinase production of phosphatidylinositol 4,5 bisphosphate. PA stimulates phosphatidylinositol-4-phosphate 5 kinase and conversely phosphatidylinositol 4,5 bisphosphate stimulates PLD. The net effect is believed to be a feed-forward mechanism that produces brief local spikes of these two signaling molecules.<sup>8</sup> PLD2 has also been shown to participate directly in G protein-coupled receptor and tyrosine kinase receptor signaling pathways, including the metabotropic glutamate receptor and the EGF receptor.<sup>9,10</sup> Both PLD1 and PLD2 interact with a variety of cellular proteins, including ARF and rho, which modulate PLD1, and EGFR, grb2 and Sos, which interact with PLD2 (refs. 3,8). The EGF receptor is a receptor tyrosine kinase that in the presence of ligand activates the Ras, Raf, Mek, Erk, and Elk pathway as well as others.<sup>8</sup>

**Correspondence:** Nicholas Muzyczka, Department of Molecular Genetics and Microbiology, College of Medicine, UF Genetics Institute, Gene Therapy Center, Cancer/Genetics Research Complex, Building 1376, 1376 Mowry Rd, Rm CG-208, Gainesville, Florida 32610, USA. E-mail: [muzyczka@mgm.ufl.edu](mailto:muzyczka@mgm.ufl.edu) or Oleg Gorbatyuk, Department of Molecular Genetics and Microbiology, College of Medicine, UF Genetics Institute, Gene Therapy Center, Cancer/Genetics Research Complex, Building 1376, 1376 Mowry Rd, Rm CG-208, Gainesville, Florida 32610, USA. E-mail: [olegor@ufl.edu](mailto:olegor@ufl.edu)

Interestingly, some of the members of this signaling pathway, Elk and Ras, have also been shown to interact with  $\alpha$ -syn.<sup>11</sup> Finally, conversion of PC to PA essentially makes the membrane more fluid and produces negative curvature on the inner leaflet of the membrane.<sup>12</sup> This is believed to be a key step in vesicle formation in the Golgi, for endocytosis of receptors and for exocytosis. Additionally, PLD2 has been shown to activate the GTPase of dynamin by a lipase-independent mechanism.<sup>13</sup> This in principle could modulate the rate of endosome formation.

The two isoforms of PLD share most cellular locations, but it is believed that PLD1 is involved in vesicle formation in the Golgi and PLD2 is predominantly located in the cell membrane.<sup>3</sup> Both of these locations have also been implicated in  $\alpha$ -syn function.<sup>1</sup> The N-terminal 330 aa of PLD2, containing the phox and pleckstrin domains, are responsible for many of the protein interactions so far discovered, including dynamin,<sup>13</sup> Grb2 (ref. 9), and EGFR,<sup>10</sup> as well as the interaction with  $\alpha$ -syn.<sup>4</sup> Thus,  $\alpha$ -syn binding to PLD2 could inhibit the binding of some or all of these PLD partners. PLD2 is expressed in most regions of the mouse brain, including the substantia nigra pars compacta (SNc) and striatum (see Allen Mouse Brain Atlas: <http://mouse.brain-map.org/brain/Pld2.html?ispopup=true>).

To date, no knockout or transgenic models of PLD have been reported. In this report, we use viral-mediated gene transfer to rat SNc to examine the effect of overexpression or knockdown of PLD2. We show that the level of PLD2 in DA neurons appears to be critical. Overexpression of PLD2 leads to loss of DA in the striatum, nigral neurodegeneration, and amphetamine-induced rotational asymmetry. Moreover, we show that when both PLD2 and  $\alpha$ -syn are coexpressed in rat SNc,  $\alpha$ -syn suppresses PLD2 toxicity. Further, knockdown of PLD2 by siRNA results in the same unusual contralateral amphetamine-induced rotational behavior as expression of  $\alpha$ -syn. These results are consistent with a primary role for  $\alpha$ -syn being the modulation of PLD activity, and suggest that PLD may be a novel target for treating Parkinson disease.

## RESULTS

### Efficient expression of multiple genes in rat SNc

The rat *PLD2* gene was fused to an N-terminal HA epitope and cloned into a recombinant adeno-associated virus (rAAV) vector. Rats injected with rAAV virus-expressing PLD2 were then compared with those injected with green fluorescent protein (GFP),  $\alpha$ -syn alone, and a mixture of PLD2 + human wt  $\alpha$ -syn or the  $\alpha$ -syn mutant S129D. All of the genes engineered into rAAV vectors were expressed from the same chicken  $\beta$ -actin cytomegalovirus hybrid promoter.

Only the SNc on the right side of the brain was injected; the left side was used as an uninjected control. As expected, immunoblotting of SNc and striatal tissue extracts with HA antibody (Figure 1a) and immunocytochemistry of SNc (Figure 2a) showed expression of HA-PLD2 fusion protein only on the side that was injected. Because DA neurons in the SNc project axons to the striatum where DA is released, the presence of HA-tagged PLD2 in the striatum demonstrated that PLD2 was transported anterogradely to SNc presynaptic junctions in the striatum. Examination of tissue extracts with an antibody specific for rat PLD2 demonstrated that there was at most a twofold increase in

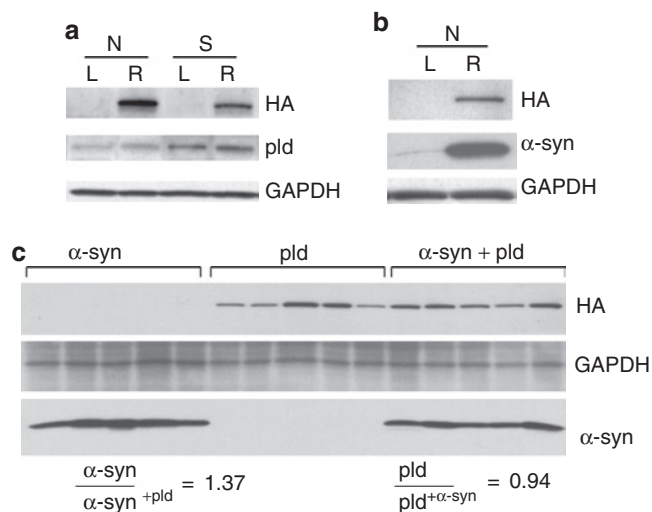


**Figure 1** Expression of exogenous HA-tagged rat PLD2 or human  $\alpha$ -syn in rats injected with rAAV expression vectors. **(a)** Nigral (N) or striatal (S) tissue from 4-week animals was extracted and pooled ( $n = 5-7$ ) and then immunoblotted with antibody to the HA epitope (HA) or to rat PLD2 (pld). A loading control (GAPDH) is also shown. Extracts from the uninjected side (L) were compared with the injected side (R). Only the injected side expressed the HA-tagged exogenous PLD2. An immunoblot with PLD2 antibody (pld) showed an approximately twofold increase in total PLD2 in both SNc (N) and striatum (S). **(b)** Nigral tissues from four animals injected with both the rat PLD2 and human  $\alpha$ -syn expression vectors were pooled 4 weeks after injection and immunoblotted with both HA antibody and antibody to human  $\alpha$ -syn. Both proteins were expressed only on the injected side. **(c)** Nigral tissue extracts from 4-week animals injected with PLD2,  $\alpha$ -syn, or PLD2+ $\alpha$ -syn were immunoblotted sequentially with antibodies to HA,  $\alpha$ -syn, or GAPDH. Five animals from each group are shown. Antibody signals were measured by fluorescent scanning, normalized to GAPDH, and the mean ratio of PLD2 compared to PLD2 in the presence of  $\alpha$ -syn was calculated to be 0.94. The  $\alpha$ -syn to  $\alpha$ -syn + PLD2 ratio was similarly calculated (mean = 1.37).

total intracellular PLD2 activity in SNc (Figure 1a). Essentially, no increase was seen in striatal tissues, presumably due to the large background of striatal cells that had not been targeted for injection. On higher resolution gels, a similar twofold increase was seen in SNc tissue when rat PLD2 antibody was used to compare endogenous PLD2 levels that had been separated from the higher molecular weight HA epitope-tagged protein (data not shown). The level of  $\alpha$ -syn-expressing vector used was identical to that used previously<sup>5</sup> and had been shown to produce an approximately 3.5-fold increase in total  $\alpha$ -syn in SNc. Rats injected with human  $\alpha$ -syn expression vectors, expressed human  $\alpha$ -syn only on the injected side as expected (Figure 1b).

All of the vectors contained AAV5 serotype capsids. These had been shown by us and others<sup>14-17</sup> to transduce virtually all of the neurons in the rat SNc (>95%) at the input dose used in these studies. In addition to neurons of the SNc, neurons in the immediate surrounding area, including the ventral tegmental area, were also transduced (Figure 2). As shown previously, AAV5 serotype vectors transduce predominantly neurons rather than astrocytes<sup>14-17</sup> and produce little if any inflammatory response or gliosis.<sup>18,19</sup> Thus, the phenotypes observed in this study are due primarily to genetic changes in the neurons of the SNc rather than nonspecific effects due to virus injection or transduction of astrocytes. Unlike the



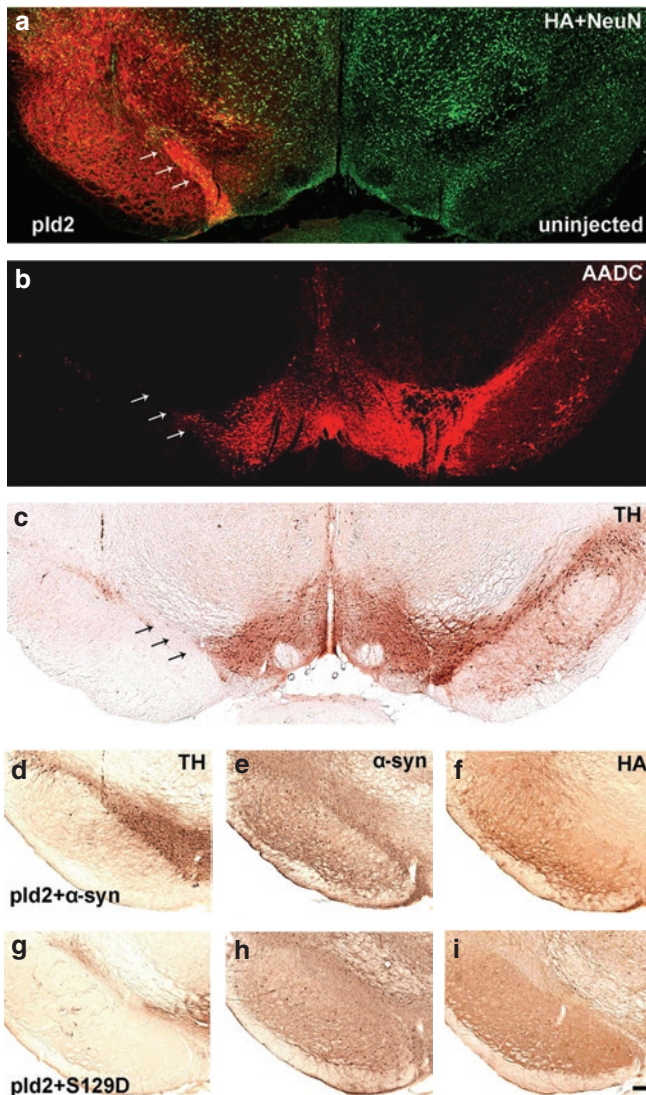


**Figure 2** Microscopic images showing the SNc at 8 weeks after injection of (a–c) PLD2 alone, or in combination with (d–f) human wt  $\alpha$ -syn or (g–i) S129D. (a) Confocal image of SNc tissue expressing HA-tagged PLD2 and stained with NeuN (green) and HA (red) antibody. HA-PLD2 expression is seen only on the injected side. A few NeuN positive cells can be found in SNc on the injected side (arrows). (b) AADC staining of neighboring section shown in a showing severe cell loss on side injected with PLD2-expressing virus. (c) TH-immunoperoxidase labeling on a neighboring section of the nigral region shown in a, injected with HA-PLD2 vector, revealed severe cell loss in the same area of the SNc (arrows) compared to the uninjected side. (d–f) TH-,  $\alpha$ -syn-, and HA-immunoperoxidase staining of SNc injected with PLD2 + wt  $\alpha$ -syn shows expression of both PLD2 and  $\alpha$ -syn, but no significant loss of TH<sup>+</sup> neurons. (g–i) TH-,  $\alpha$ -syn-, and HA-immunoperoxidase staining of SNc injected with PLD2 + S129D rAAV shows less expression of  $\alpha$ -syn and PLD2, presumably because most of the TH<sup>+</sup> neurons are lost. Bar = 150  $\mu$ m.

more commonly used AAV2 serotype, AAV5 does not bind to cell surface heparan sulfate proteoglycans; thus, a lower dose of AAV5 is able to spread throughout a larger volume of the SNc and results in a lower copy number of the transgene per SNc neuron.<sup>14–16</sup>

One concern during these experiments was that co-injection of more than one vector might affect the expression of one or the other gene. Animals injected with both PLD2 and  $\alpha$ -syn showed

expression of both proteins on the injected side (Figure 1b,c and Figure 2d–f). Co-injection of two different viruses expressing PLD2 and  $\alpha$ -syn did not have a significant effect on the expression level of either protein (Figure 1c). When antibody signals were normalized to GAPDH, the level of PLD2, when injected alone was essentially the same as when injected with  $\alpha$ -syn (Figure 1c). The ratio of PLD2 in the two experiments was close to one (PLD2/PLD2+ $\alpha$ -syn = 0.94, n = 5). Similarly, the ratio of  $\alpha$ -syn, when injected alone, compared to  $\alpha$ -syn + PLD2 was a mean of 1.37 (Figure 1c, n = 5). Additional control experiments were done with mixtures of GFP virus and empty capsids as well as GFP virus and virus carrying a null gene. These experiments confirmed that no inhibition of GFP expression was seen that might be due to viral competition for cell binding or cell entry (data not shown). We concluded that it was feasible to express two different genes in >90% of SNc neurons by co-infecting with two vectors without significant interference between the vectors.

**PLD2 overexpression in SNc results in neurodegeneration and  $\alpha$ -syn is an *in vivo* inhibitor of PLD2 toxicity**

Expression of PLD2 caused a severe loss of TH<sup>+</sup> neurons in the SNc at 8 weeks after injection (Figure 2c, arrows). Unbiased estimation of nigral TH<sup>+</sup> cells revealed a severe pathology at 4 weeks that progressed to over 80% loss of TH<sup>+</sup> neurons at 8 weeks (Figure 3a,b). A similar loss of TH neurons was seen when sections were stained for aromatic amino acid decarboxylase (AADC) (compare Figure 2b,c, arrows) or cresyl violet (data not shown). This suggested that TH<sup>+</sup> cell loss was not simply due to downregulation of TH expression and confirmed that most of the SNc neurons had been transduced with PLD2 virus. However, if PLD2 was coexpressed with wt human  $\alpha$ -syn, the level of degeneration was essentially the same as that seen with  $\alpha$ -syn alone, *i.e.*,  $\alpha$ -syn suppressed PLD2 toxicity (Figure 2, compare C (arrows) and D). At 8 weeks after vector administration, there was no significant difference between  $\alpha$ -syn and PLD2 +  $\alpha$ -syn groups, and both were significantly different from PLD2 alone (Figure 3a, compare  $\alpha$ -syn, pld2+ $\alpha$ -syn and pld2). This suggested that  $\alpha$ -syn is an inhibitor of PLD2 *in vivo*.

$\alpha$ -syn with a substitution of an acidic amino acid for ser129 has been shown to be defective for PLD2 lipase inhibition *in vitro*.<sup>7</sup> We reasoned that if  $\alpha$ -syn is an inhibitor of PLD2 *in vivo*, and phospholipase activity is necessary for toxicity, then  $\alpha$ -syn containing the S129D substitution should be incapable of suppressing PLD2 neurodegeneration. Indeed, when we mixed S129D with PLD2, we saw almost no difference in the fraction of TH<sup>+</sup> cells surviving compared to PLD2 alone, indicating that S129D did not inhibit PLD2-induced nigral toxicity (Figure 3a and Figure 2, compare d and g). S129D alone, however, showed no toxicity at the 8-week time point as shown previously by us and others (Figure 3a).<sup>5,6</sup> Thus, S129D did not inhibit PLD2-induced toxicity *in vivo*. The fact that the level of degeneration seen in PLD2 and PLD2 + S129D animals was essentially the same, and similarly, the extent of neurodegeneration in PLD2 + wild-type  $\alpha$ -syn and wild-type  $\alpha$ -syn animals was the same (Figure 3a,b), is consistent with earlier *in vitro* reports that  $\alpha$ -syn is an inhibitor of PLD2 (refs. 2,4,7).

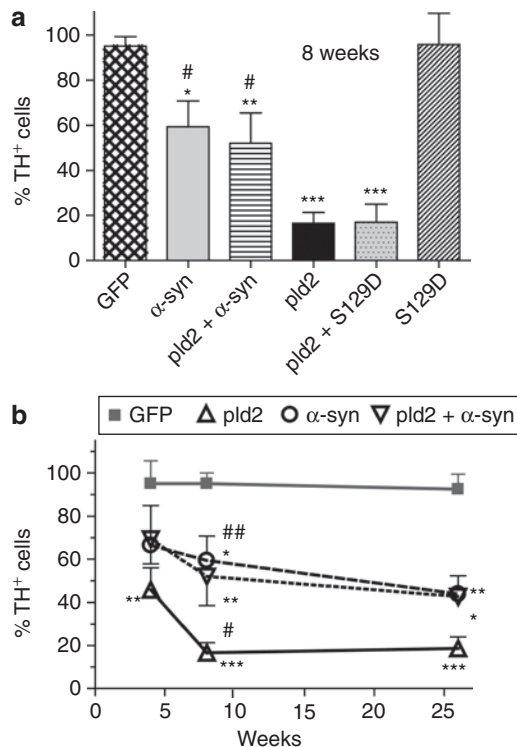


**Figure 3** Unbiased estimation of TH<sup>+</sup> cells remaining in SNc. **(a)** The percentage of TH<sup>+</sup> cells at 8 weeks after injection was calculated by comparison with the uninjected side in the same animal. One-way group analysis of variance (ANOVA) statistics for 8 weeks were as follows:  $F[4,37] = 18.07$ ,  $P = 0.0001$ . Tukey's *post hoc* results are indicated as \* $P < 0.05$ , \*\* $P < 0.01$ , and \*\*\* $P < 0.001$  versus GFP; # $P < 0.05$ , ## $P < 0.01$ , ### $P < 0.001$  versus pld2.  $N = 4-8$  per group. **(b)** Time course of TH<sup>+</sup> cell survival at 4, 8, and 26 weeks. Eight-week animals were the same as in **a**. Two-way ANOVA statistics (TIME versus GENE) were for TIME:  $F[2,58] = 3.457$ ,  $P = 0.0382$ ; and for GENE:  $F[3,58] = 19.11$ ,  $P = 0.0001$  with no interaction between TIME and GENE:  $F[6,58] = 0.4626$ ,  $P = 0.8331$ . Bonferroni post-tests are indicated as \* $P < 0.05$ , \*\* $P < 0.01$ , \*\*\* $P < 0.001$  versus GFP; and # $P < 0.05$ , ## $P < 0.01$  versus pld2;  $N = 4-15$  per group. Asterisks indicate that the group is being compared to the GFP group at the same time point. Number signs (#) mean that the group is being compared to the pld2 group at the same time point. Solid squares plus gray line represent GFP, open triangle + black line represent PLD2, open circle plus dashed line represent human  $\alpha$ -syn, and inverted open triangle + dotted line represent  $\alpha$ -syn + PLD2.

Inhibition of PLD2 toxicity by  $\alpha$ -syn was tested at three time points, 4, 8, and 26 weeks after injection. Essentially, the same relationships were seen over all three time points tested between different vector treatment groups (**Figure 3b**). There was no TIME  $\times$  GENE interaction, but there was a clear progressive loss of neurons with time. The number of TH<sup>+</sup> neurons was essentially the same at all time points for  $\alpha$ -syn and  $\alpha$ -syn + PLD2 (**Figure 3b**). We also measured the amount of DA in the striatum of all animals (**Supplementary Figure S1a**). In general, the levels of striatal DA on the injected side agreed with the estimated surviving TH<sup>+</sup> cells at each time point (compare **Figure 3a** and **Supplementary Figure S1a**); however, it appeared that loss of DA in the striatum was not as efficiently suppressed as loss of TH<sup>+</sup> cells by  $\alpha$ -syn expression. This may be due to the fact that increases in  $\alpha$ -syn can also inhibit TH activity by an alternative mechanism.<sup>20</sup>

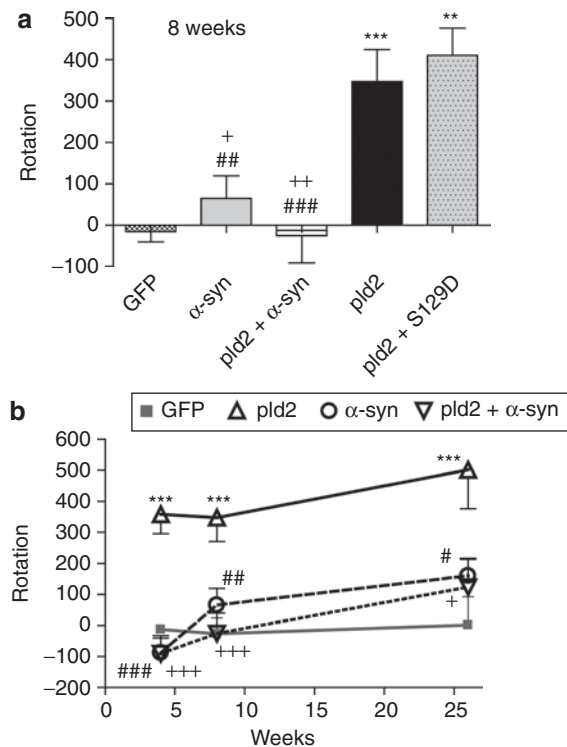


**Figure 4** Effect of PLD2 on amphetamine-induced rotation. **(a)** Amphetamine-induced rotation at 8 weeks after injection was measured for 90 minutes, and the means of cumulative totals plus SE are shown. One-way analysis of variance (ANOVA) analysis was as follows:  $F[4,85] = 10.81$ ,  $P = 0.0001$ .  $N = 4-41$  per group. Tukey *post hoc* results are indicated as in previous figure: one symbol  $P < 0.05$ , two symbols  $P < 0.01$ , and three symbols  $P < 0.001$ . \*Comparison with GFP group, #comparison with pld2 group, and +comparison with pld2+S129D group. There was no significant difference between the human  $\alpha$ -syn group or the human  $\alpha$ -syn + PLD2 group and the GFP group. **(b)** Amphetamine rotation versus time after injection. Two-way ANOVA statistics for TIME are as follows:  $F[2,139] = 4.532$ ;  $P = 0.0124$ ; for GENE:  $F[3,139] = 21.88$ ,  $P = 0.0001$ , for TIME  $\times$  GENE interaction:  $F[6,139] = 0.8976$ ,  $P = 0.8986$ . Bonferroni post-test is indicated as one symbol  $P < 0.05$ , two symbols  $P < 0.01$ , and three symbols  $P < 0.001$ ;  $N = 4-18$  per group. Asterisks indicate comparison of the PLD2 group at a particular time point with GFP at the same time point. Only PLD2 groups were significantly different from GFP groups. Number signs (#) indicate comparison of an  $\alpha$ -syn group with a PLD2 group at the same time point. Plus signs (+) indicate comparison of a PLD2 plus an  $\alpha$ -syn group with a PLD2 group at the same time point. Solid squares plus gray line represent GFP, open triangle + black line represent PLD2, open circle plus dashed line represent human  $\alpha$ -syn, and inverted open triangle + dotted line represent human  $\alpha$ -syn + PLD2.

### PLD2 expression produces a severe behavioral asymmetry

Once striatal DA level dropped below 50%, we expected to see a behavioral asymmetry in the amphetamine rotation test as had been shown for 6-OH DOPA lesions.<sup>21,22</sup> At 8 weeks after rAAV treatment, animals that expressed PLD2 rotated strongly toward the injected side (positive rotation) and the rotation was significantly different from both the GFP ( $P < 0.001$ ) and wt human  $\alpha$ -syn group (**Figure 4a**). As expected from the surviving number of TH<sup>+</sup> cells (**Figure 2a**), wt  $\alpha$ -syn essentially suppressed the PLD2-induced rotational behavior but the S129D mutant did not (**Figure 4a**). PLD2 animals showed a rotational asymmetry at



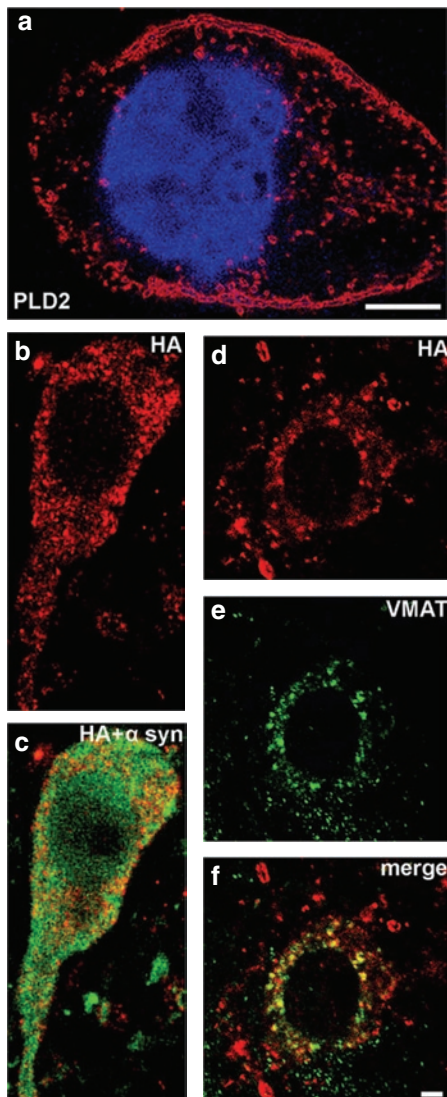


**Figure 5** Confocal microscopy of cells in the SNc of animals (a–c) 4 or (d–f) 8 weeks after injection of HA-tagged PLD2-expressing rAAV (a), or both PLD2 and  $\alpha$ -syn vectors (b–f). (a) SNc neuron expressing PLD2 (red = HA antibody, blue = DAPI) showing localization of PLD2 to membrane and intracellular vesicles. (b) SNc neuron 4 weeks after injection with HA-PLD2 and  $\alpha$ -syn that has been stained for HA (red). (c) Same as b, but stained for both HA (red) and  $\alpha$ -syn (green). (d) SNc neuron 8 weeks after injection with HA-PLD2 and  $\alpha$ -syn stained for HA (red). (e) Same as d but stained for VMAT (green). (f) Same as d but stained for both HA and VMAT. Note that PLD2 partially colocalizes with VMAT (f) and  $\alpha$ -syn (c) when  $\alpha$ -syn is coexpressed with HA-PLD2.

all time points tested and were significantly different from GFP,  $\alpha$ -syn, and  $\alpha$ -syn + PLD2 at all time points (Figure 4b). However, there was no difference between GFP and  $\alpha$ -syn, GFP and  $\alpha$ -syn + PLD2, or  $\alpha$ -syn and  $\alpha$ -syn + PLD2 treated rats at any time point (Figure 4b).

**Evidence for physical interaction between  $\alpha$ -syn and PLD2 *in vivo***

Confocal microscopy of SNc sections from animals expressing the HA-PLD2 fusion protein revealed that HA-PLD2 localized primarily to membranes and vesicles (Figure 5a), confirming

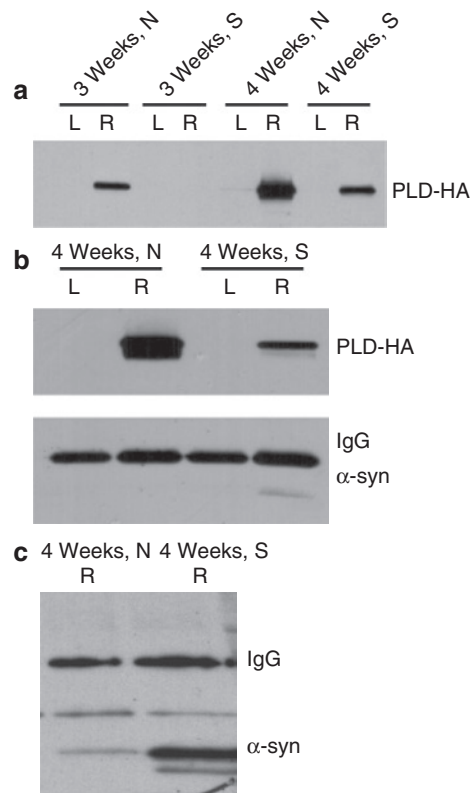


**Figure 6** Coprecipitation of  $\alpha$ -syn with PLD2 from striatal and nigral tissue. (a) Striatal (S) or nigral (N) tissue was pooled from three rats injected with vector expressing HA-tagged PLD2 at 3 or 4 weeks after injection and probed with HA antibody to detect vector-expressed PLD2. L represents uninjected and R represents injected hemispheres. PLD expression appears in nigral cell bodies by 3 weeks but not until 4 weeks in nigral synapses in striatal tissue. (b,c) At 4 weeks, extracts were prepared from nigral or striatal tissues from animals injected with HA-tagged PLD2 and human  $\alpha$ -syn vectors. The extracts were precipitated with anti-HA antibody and probed with anti-HA and anti- $\alpha$ -syn antibody (b) or just  $\alpha$ -syn antibody (c).  $\alpha$ -syn coprecipitates with PLD2 from striatal tissue but at a lower level from nigral tissue. b and c show variation in amounts of  $\alpha$ -syn immunoprecipitated with HA antibody.

previous reports.<sup>23</sup> Immunostaining for both HA and vesicular monoamine transporter (VMAT) showed colocalization consistent with the presence of PLD2 in perinuclear vesicles (Figure 5d–f). PLD2 also partially colocalized with human  $\alpha$ -syn when the two genes were coexpressed (Figure 5b,c).

rAAV-mediated gene expression has been shown to peak between 3 and 4 weeks in brain tissue,<sup>19</sup> and PLD2-induced cell death was not yet complete at these time points (Figure 3b). Because nigral neurons had not completely degenerated at these time points, we harvested striatal and nigral tissues from animals injected with HA-tagged PLD2 at 3 and 4 weeks after injection to see whether we could demonstrate a direct interaction between PLD2 and human  $\alpha$ -syn *in vivo*. HA-PLD2 could be detected in nigral but not striatal tissues at 3 weeks (Figure 6a). By 4 weeks, a large fraction of the total HA-PLD2 had localized to striatal synapses, demonstrating that PLD2 protein had been transported in anterograde fashion from the site of expression in SNc. When HA antibody was used to immunoprecipitate exogenously expressed HA-PLD2 from nigral or striatal tissues, and probed for

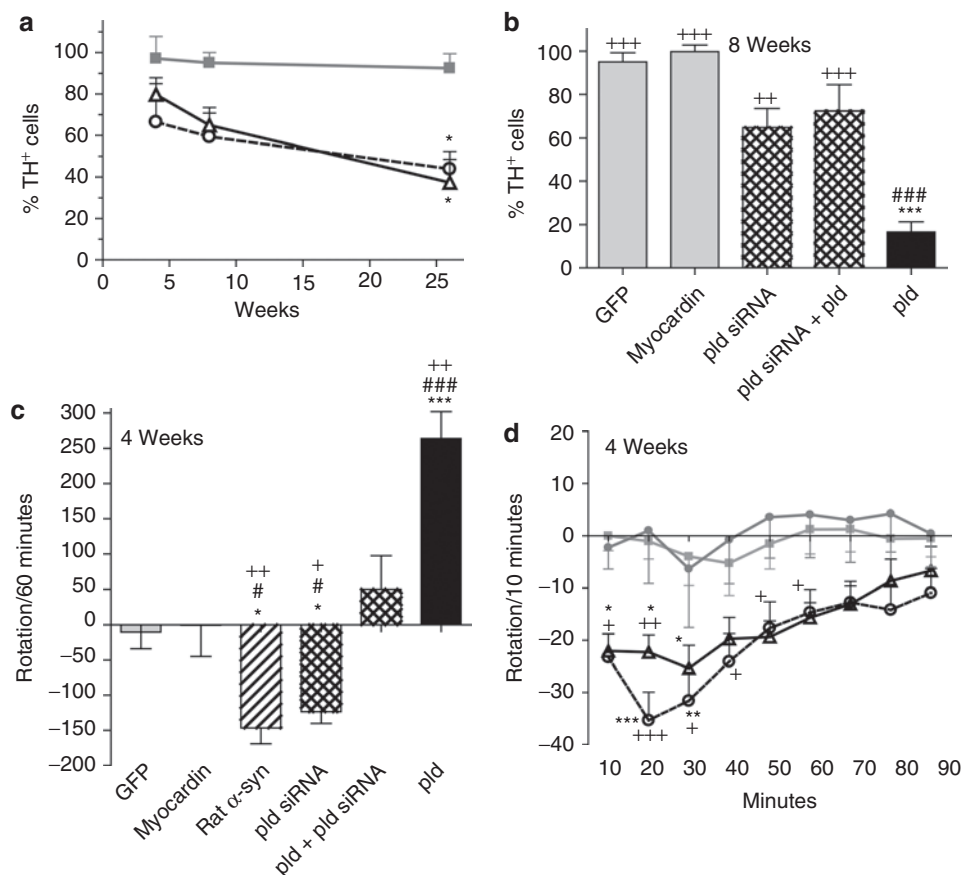


**Figure 7** Comparison of the effect of PLD2 siRNA and  $\alpha$ -syn expression on SNc neuron survival and rotational behavior. **(a)** Unbiased estimation of TH<sup>+</sup> cells remaining in SNc on the injected side as a percentage of the uninjected side + SE at different times after injection of PLD2 siRNA or human  $\alpha$ -syn. Both PLD2 siRNA and human  $\alpha$ -syn animals show a nearly identical progressive loss of TH<sup>+</sup> neurons over a 26-week time course. (See **Supplementary Figure S1b** for a time course of DA loss in these animals and **Supplementary Figure S4** for additional comparisons with myocardin.) Two-way analysis of variance (ANOVA) statistics (TIME versus GENE) were for TIME:  $F[2,41] = 3.48$ ,  $P = 0.040$ ; and for GENE:  $F[2,41] = 11.24$ ,  $P = 0.0001$  with no interaction between TIME and GENE:  $F[4,41] = 0.721$ ,  $P = 0.583$ . Bonferroni post-tests are indicated as \* $P < 0.05$  for  $\alpha$ -syn or PLD2 siRNA versus GFP at the 26-week time point; no other group comparisons at each time point were significant;  $N = 4-8$  for each group at each time point. Gray squares represent GFP virus; open triangles represent PLD2 siRNA; open circles represent rat  $\alpha$ -syn. **(b)** PLD2 toxicity is suppressed by PLD2 siRNA. The graph shows the % TH<sup>+</sup> cells remaining in cells expressing PLD2 versus PLD2 + PLD2 siRNA at 8 weeks after injection. At this time point, PLD2 siRNA and PLD2 + PLD2 siRNA groups are not significantly different from control GFP and myocardin siRNA groups. All groups, however, are significantly different from animals injected with PLD2 alone (+ symbols), suggesting that PLD2 siRNA is specific for PLD2. One-way ANOVA analysis was  $F[4,33] = 24.46$ ,  $P < 0.0001$ . Tukey *post hoc* results are indicated as follows: two symbols =  $P < 0.01$ , three symbols =  $P < 0.001$ .  $N = 4-8$  per group. \*Comparison with GFP group, #comparison with myocardin siRNA, and +comparison with PLD2 group. **(c)** Cumulative 60-minute amphetamine-induced rotation toward the injected side (positive, ipsilateral rotation) or uninjected side (negative, contralateral rotation) in animals injected with virus expressing rat  $\alpha$ -syn or PLD2 siRNA at 4 weeks after injection. At 4 weeks, the number of TH<sup>+</sup> cells **(a)** and striatal DA (**Supplementary Figure S1c**) on the injected side are not significantly different from the uninjected control side. However, both rat  $\alpha$ -syn and rat PLD2 siRNA animals show contralateral (negative) rotation when treated with amphetamine compared to both GFP and myocardin siRNA controls. One-way ANOVA analysis was  $F[5,69] = 24.55$ ,  $P < 0.0001$ .  $N = 5-25$  per group. Comparison between groups using Tukey *post hoc* is indicated as follows: one symbol =  $P < 0.05$ , two symbols =  $P < 0.01$ , and three symbols =  $P < 0.001$ . \*Comparison with GFP group, #comparison with myocardin siRNA, and +comparison with PLD2+PLD2 siRNA group. Absence of a symbol indicates that the comparison was not statistically significant, e.g., the PLD2+PLD2 siRNA group was not significantly different from GFP and myocardin controls. **(d)** Time course of amphetamine-induced rotation in animals injected with virus expressing GFP (filled squares), control myocardin siRNA (filled circles), PLD2 siRNA (open triangles), or rat  $\alpha$ -syn (open circles). Both rat  $\alpha$ -syn- and PLD2 siRNA-injected animals show a similar time course of contralateral rotation compared to myocardin siRNA and GFP. Two-way ANOVA statistics for TIME:  $F[8,448] = 6.32$ ,  $P < 0.0001$ ; GENE:  $F[3,448] = 6.37$ ,  $P = 0.0009$ ; for TIME  $\times$  GENE interaction:  $F[24,448] = 1.217$ ,  $P = 0.22$ .  $N = 11-25$  per group. Asterisks indicate comparison to GFP at each time bin, + indicates comparison to myocardin siRNA at each time bin. One, two, or three symbols indicate  $P < 0.05$ ,  $P < 0.01$ , or  $P < 0.001$ , respectively.

coprecipitation of  $\alpha$ -syn, only tissues from the striatum showed significant coimmunoprecipitation of  $\alpha$ -syn (**Figure 6b,c**). We also noted that, although  $\alpha$ -syn was consistently coprecipitated with PLD2, the levels of  $\alpha$ -syn varied from experiment to experiment (compare **Figure 6b,c**). Taken together, the confocal data

and coimmunoprecipitation experiments both suggested that a significant amount of  $\alpha$ -syn was present in a complex with PLD2. Moreover, the immunoprecipitation experiments suggested that complex formation occurred primarily in striatal synapses, suggesting that this was the site of functional interaction.

### Reduction of PLD2 by siRNA or by $\alpha$ -syn expression both produce the same unusual behavioral deficit

We noticed that at 4 weeks after injection of human  $\alpha$ -syn or human  $\alpha$ -syn + PLD2, injected animals appeared to rotate contralateral to the injected side compared to GFP controls (**Figure 4b** and **Supplementary Figure S2**). Although not statistically significant when compared to GFP controls, the trend was consistently present at early time points (4 weeks) for all wt human  $\alpha$ -syn injected animals.

To see whether this effect was due to inhibition of PLD, we identified a PLD2 siRNA that was effective in reducing the level of HA-tagged PLD2 in cell culture by ~90% (see Methods). When the PLD2 siRNA was injected *in vivo* into SNc, endogenous PLD2 mRNA was reduced by ~50% at 4 weeks after injection as judged by RT-PCR for mRNA (**Supplementary Figure S3a**) and the effect on PLD1 was not significant. The reduction of PLD2 protein levels in both striatum and nigra was also ~50% as judged by immunoblotting with PLD2 antibody (**Supplementary Figure S3b**). As an *in vivo* control, we used an siRNA directed to the myocardin gene, which is normally not expressed in brain tissues. We also cloned the rat  $\alpha$ -syn gene into a rAAV vector containing the same expression cassette that was used for human  $\alpha$ -syn (see Methods) to see whether the behavioral effect was common to both species of  $\alpha$ -syn.

When a rAAV vector expressing the PLD2 siRNA was injected into rat SNc, the level of degeneration seen was comparable to that seen with human wt  $\alpha$ -syn, and followed approximately the same time course (**Figure 7a**, **Supplementary Figure S4**). By 26 weeks after injection, both treatment groups had lost 55–60% of the TH<sup>+</sup> neurons, whereas the GFP and myocardin siRNA controls showed no significant loss of TH<sup>+</sup> neurons. There was no significant difference between animals injected with both PLD2 siRNA and  $\alpha$ -syn and the groups that were injected with PLD2 siRNA or  $\alpha$ -syn alone (**Supplementary Figure S4**). The steady-state level of DA in the striatum as a function of time in groups injected with PLD2 siRNA and  $\alpha$ -syn was also similar (**Supplementary Figure S1c**). Although both human  $\alpha$ -syn and rat PLD2 siRNA produced detectable loss of TH<sup>+</sup> cells and DA at 4 weeks after injection, neither reached statistical significance at this time point (**Figure 7a**, **Supplementary Figure S1c**). Similarly, injection of vector expressing wild-type rat  $\alpha$ -syn also induced no significant loss of TH<sup>+</sup> neurons at 4 weeks after injection (data not shown).

When we examined amphetamine-induced rotational behavior at 4 weeks, both rat  $\alpha$ -syn and PLD2 siRNA vectors produced the same contralateral rotational behavior seen with human  $\alpha$ -syn (**Figure 7c**, compare with **Supplementary Figure S2**). The effect was statistically significant when compared to GFP-injected animals and animals injected with the control myocardin expressing siRNA. In addition, the time course of rotational asymmetry was the same for both PLD2 siRNA and rat  $\alpha$ -syn (**Figure 7d**). The contralateral rotation was also seen in animals injected with PLD2 siRNA at 8 weeks (**Supplementary Figure S5**). However, the effect was no longer statistically significant with the number of animals tested, presumably because the number of TH<sup>+</sup> neurons had decreased by 8 weeks. In contrast to the contralateral rotation induced in animals injected with PLD2 siRNA or rat  $\alpha$ -syn, injection with PLD2-expressing vector produced the opposite effect, a pronounced ipsilateral (positive) rotation at this early time point

(**Figure 7c**). This occurred even though >50% of the striatal DA remained (**Supplementary Figure S1b**), which would normally not produce asymmetric rotation due to loss of DA. The ipsilateral rotation in 4-week PLD2 animals is also reversed by co-injection with  $\alpha$ -syn (**Figure 4b**, see 4-week time point). Thus, the level of PLD2 activity appears to be critical for determining the direction of asymmetry induced by amphetamine. Finally, the effect of PLD2 siRNA appeared to be reversed by coexpression of PLD2 (**Figure 7c**), suggesting that the siRNA was specifically targeting endogenous rat PLD2. This was confirmed by examining the effect of PLD2 siRNA on the neurodegeneration seen with PLD2. When PLD2 siRNA-expressing virus was co-injected with PLD2 virus, neurodegeneration was suppressed at the 8-week time point (**Figure 7b**). There was no significant difference between the GFP, myocardin, PLD2 siRNA and PLD2 siRNA + PLD2 groups, and all of these groups were significantly different from PLD2 alone (**Figure 7b**).

The unusual negative rotation (rotation away from the injected side) suggests an increased steady-state level of DA signaling on the injected side (compared to the uninjected side) after amphetamine treatment. This is presumably due either to increased release, slower reuptake, or slower repackaging of DA on the injected side. Notably, reduction of PLD2 by siRNA and overexpression of rat  $\alpha$ -syn appeared to produce the same unusual rotational asymmetry. This provided additional evidence that  $\alpha$ -syn interacts with PLD2 *in vivo*.

## DISCUSSION

### Increase in PLD2 expression in SNc is toxic

Our results demonstrate that modest overproduction of PLD2 (twofold) induces a severe nigrostriatal degeneration. Furthermore, simultaneous expression of  $\alpha$ -syn negatively modulates these effects. The implication of these results is that at least one of the biological functions of  $\alpha$ -syn is to inhibit PLD2 activity *in vivo*. Our data also demonstrate that it is possible to use viral-mediated gene transfer to study the interaction of two genes.

Expression of PLD2 induced a rapid loss of TH<sup>+</sup> cells in SNc; within 2 months after injection, >80% of DA neurons were lost (**Figures 2** and **3**). Given that rAAV vectors do not reach full expression until 3–4 weeks after injection,<sup>19</sup> this suggests that a modest increase in PLD2 causes an acute toxicity that leads to cell death. The loss of cells was confirmed by multiple markers (TH, AADC, and cresyl violet) and confirmed that most, if not all, SNc neurons had been transduced with recombinant virus. Consistent with the loss of DA neurons, we saw an equally severe loss of striatal DA and a pronounced ipsilateral amphetamine-induced rotation (**Figure 4** and **Supplementary Figure S1**). A curious aspect of the rotational asymmetry was that it became pronounced at 4 weeks (**Supplementary Figure S2**), when DA neurons were still present and before striatal DA loss had reached 50% (data not shown). This suggested that an immediate biochemical effect of increased PLD2 might be to inhibit DA release. In this regard, we have not yet tested whether the toxicity of PLD2 expression is unique to DA neurons or is common to all neurons.

### PLD2 toxicity is modulated by $\alpha$ -syn *in vivo*

Several lines of evidence support the *in vivo* interaction of PLD2 and  $\alpha$ -syn. First, loss of TH<sup>+</sup> cells due to PLD2 overexpression



is largely reversed by expression of  $\alpha$ -syn. For over half a year after injection, loss of DA neurons in the presence of PLD2 and human  $\alpha$ -syn is virtually the same as that seen with human  $\alpha$ -syn alone (Figure 3). Furthermore, at all time points, the rotational asymmetry is completely reversed and is similar to that seen with  $\alpha$ -syn alone (Figure 5b). Only striatal DA content is incompletely reversed by  $\alpha$ -syn expression (Supplementary Figure S1).

Second, Payton *et al.*<sup>7</sup> have demonstrated that an acidic substitution at amino acid position 129 in  $\alpha$ -syn is defective for inhibiting PLD2 activity *in vitro*. This mutation mimics a commonly seen phosphorylation of this residue *in vivo*. Consistent with this, we show that expression of the  $\alpha$ -syn mutant S129D is completely defective for suppressing PLD2-induced neuronal loss and rotational asymmetry (Figure 3a).

Third, a direct physical interaction between exogenously expressed human  $\alpha$ -syn and HA-tagged PLD2 could be demonstrated by antibody coimmunoprecipitation (Figure 6). Notably, the two proteins were coprecipitated more readily from striatal tissue than nigral tissue suggesting that  $\alpha$ -syn and PLD2 form a complex primarily near synaptic junctions.

Finally, both rat  $\alpha$ -syn expression and PLD2 siRNA produced an unusual amphetamine-induced contralateral rotation, consistent with increased DA signaling in the treated hemisphere (Figure 7c,d). The PLD2 siRNA rotational effect was completely suppressed by co-injection of PLD2 (Figure 7c), and similarly, PLD2-induced neurodegeneration was inhibited by PLD2 siRNA (Figure 7b), both observations demonstrating the specificity of the PLD2 siRNA for PLD2. Previous work has shown a modest increase in ipsilateral rotation at late times after injection (26 weeks) when the loss of TH<sup>+</sup> neurons approaches 50% following injection with human  $\alpha$  syn;<sup>24</sup> however, this does not usually reach statistical significance (see Figure 4b). Presumably, this is due to the loss of DA that results from  $\alpha$ -syn-induced neurodegeneration. The contralateral rotation was observed at 4 weeks after injection when no significant changes in cell number or DA content had occurred (Figure 7a, Supplementary Figure S1b). The fact that no significant change in DA content was detected at 4 weeks suggests that the rotational asymmetry was likely due to altered DA reuptake or vesicle packaging.

It is worth noting also that reduction of PLD2 with siRNA appeared to cause the same slow progressive neurodegeneration that was seen with overexpression of human  $\alpha$ -syn alone (Figure 7a and Supplementary Figure S4). Co-injection of  $\alpha$ -syn and PLD2 siRNA produced a slightly accelerated neurodegeneration that was not significantly different from injection of either vector alone. This suggests the intriguing possibility that expression of  $\alpha$ -syn could lead to progressive neurodegeneration through reduction of PLD2, and that both reduction of PLD2 and increase of PLD2 are pathogenic. Several groups, however, have shown that vector-mediated expression of siRNAs may have off-target toxic effects.<sup>25,26</sup> Although it is clear that the PLD2 siRNA specifically reduces the level of endogenous rat PLD2 (Supplementary Figure S3), until additional PLD2 and control siRNAs are tested, we cannot be certain that the PLD2 siRNA did not also affect additional genes that resulted in the long-term toxicity seen at 6 months after injection (Figure 7a, Supplementary Figure S4).

Taken together, these lines of evidence strongly suggest that  $\alpha$ -syn functionally interacts with PLD2 *in vivo* and is necessary to modulate its activity. A puzzling aspect of the interaction is that  $\alpha$ -syn coexpression does not completely eliminate PLD2-induced neurodegeneration. In spite of the fact that  $\alpha$ -syn expression inhibits the neurodegeneration due to PLD2, we continue to see a slow neurodegeneration that is seen with  $\alpha$ -syn alone. By 6 months, we, as well as other groups that expressed wild-type human  $\alpha$ -syn, had lost ~50% of the DA neurons.<sup>5,24,27</sup> This suggests that  $\alpha$ -syn can independently promote neurodegeneration by a mechanism unrelated to PLD2 inhibition. Many groups have suggested that  $\alpha$ -syn aggregation is toxic through a variety of mechanisms and our data is consistent with this possibility. However, given that reduction of PLD2 with siRNA appears to cause the same slow neurodegeneration seen with  $\alpha$ -syn overexpression, it is possible that  $\alpha$ -syn toxicity is due to reduction of PLD2.

The incomplete inhibition of PLD2 toxicity is similar to what had been seen previously with  $\alpha$ -syn suppression of toxicity due to the loss of CSP $\alpha$  (cysteine-string protein- $\alpha$ ), the only other *in vivo* gene interaction that has been demonstrated for  $\alpha$ -syn. Chandra *et al.*<sup>28</sup> have demonstrated that expression of human  $\alpha$ -syn suppressed the rapid neurodegeneration seen in CSP $\alpha$  null mice by an apparent downstream mechanism that involved lipid interaction. However, as in the PLD2 case reported here, the neurodegeneration normally induced by  $\alpha$ -syn alone continued unabated. Because we do not know the mechanism of PLD2 toxicity, it is conceivable that, like CSP $\alpha$ , suppression of PLD2 neurodegeneration by  $\alpha$ -syn occurs at some step downstream of PLD2. Two lines of evidence, however, suggest that the interaction is likely to involve direct interaction. First,  $\alpha$ -syn was immunoprecipitated by PLD2 antibody from *in vivo* extracts, and second, a mutant of  $\alpha$ -syn that previously had been shown to be defective for PLD2 inhibition *in vitro*, was also defective for suppression of PLD2 toxicity *in vivo*.

The interaction of PLD2 with  $\alpha$ -syn *in vivo* reported here is consistent with reports from three groups that demonstrated the ability of  $\alpha$ -syn to inhibit PLD2 *in vitro*.<sup>2,4,7</sup> Jenco *et al.* showed that  $\alpha$ -syn inhibited PLD2 activity *in vitro* with a  $K_i = 10$ – $20$  nmol/l.<sup>2,7</sup> Because intracellular concentrations of  $\alpha$ -syn in rodent brain are ~ $15$ – $20$  nmol/l,<sup>5,20,29</sup>  $\alpha$ -syn could function as an inhibitor of PLD2 *in vivo*. Ahn *et al.*<sup>4</sup> demonstrated that  $\alpha$ -syn binds to the N-terminal 331 aa acid fragment of PLD, which is involved in lipid and protein interactions. Thus,  $\alpha$ -syn might inhibit PLD2 by preventing binding to phospholipids, which are an essential cofactor for PLD2, or to membrane proteins that depend on interaction with PLD2. Finally, Payton *et al.*<sup>7</sup> showed that modifications of  $\alpha$ -syn, such as the phosphorylation of S129 or deletion of residues involved in  $\alpha$ -helix formation (and thus, lipid binding), reduced the ability of  $\alpha$ -syn to inhibit PLD2 activity *in vitro*. As mentioned earlier, this is consistent with our finding that the  $\alpha$ -syn 129D mutant was unable to inhibit PLD2-induced neurodegeneration (Figure 3).

In contrast, one recent report was unable to demonstrate  $\alpha$ -syn inhibition of PLD2 *in vitro*.<sup>30</sup> It is not clear why this group could not reproduce the work of three previous groups. One possibility is that they used higher (~150 fold higher) PLD2 enzyme concentration. If  $\alpha$ -syn is a competitive inhibitor of the PLD2 substrate,



this might explain the absence of inhibition. A more subtle explanation highlights the difficulty of assaying PLD2 activity both *in vitro* and *in vivo*. PLD2 requires binding to phospholipid membranes for activity (via a noncatalytic site), and  $\alpha$ -syn binds to similar membranes. Inhibition can only occur when both are present in lipid vesicles. Thus, changes in bulk lipids can eliminate  $\alpha$ -syn inhibition by reducing the effective surface concentration of the substrate, a process called surface dilution. Several groups have shown that modifying bulk lipid concentration will reduce  $\alpha$ -syn inhibition.<sup>2,7</sup>

Regardless of the mechanism of inhibition, the fact that membrane binding is essential for PLD2 enzyme activity means that it was virtually impossible to assay for changes in PLD2 activity, either in nigral or striatal tissues, after expression of  $\alpha$ -syn or PLD2 siRNA. Once a tissue extract is made, the normal *in vivo* membrane environment and enzyme/ $\alpha$ -syn/lipid stoichiometry is likely to be lost; enzyme activity then can only be measured by adding additional synthetic membrane vesicles. Moreover, it appeared that the PLD2/ $\alpha$ -syn interaction occurred primarily in striatal synapses, and thus, is context specific. We are currently trying to design enzyme substrates that could be imaged in tissue slices for the purpose of measuring enzyme activity *in situ*.

### Possible mechanisms of PLD2 toxicity

PLD2 is a constitutively expressed, ubiquitous enzyme that converts phosphatidylcholine (PC) to PA.<sup>3,12,31</sup> It requires  $\text{PI4,5P}_2$  for activity<sup>32</sup> and is active only when bound to lipid vesicles *in vitro*. Regulation of PLD function and correct cellular location appear to be controlled primarily by sequences in the N-terminal 300 or so amino acids, which contain conserved phox and pleckstrin domains and have binding sites for a variety of tyrosine receptor kinases, GTPases, and PKC, as well as phospholipids.<sup>9,10,13,33</sup>

It is not immediately clear why PLD2 overexpression is toxic to DA neurons. PLD2 has been shown to be a cofactor for the activity of a variety of receptor tyrosine kinases and G protein-coupled receptors, including the metabotropic glutamate receptor<sup>34,35</sup> and the EGF receptor.<sup>9,10</sup> PLD2 also produces PA, which is a signaling molecule involved in pathways that control a wide variety of cellular processes, including cell proliferation via Raf and cell survival via TOR.<sup>36</sup> Finally, PLD2 is directly involved in endocytosis through its interaction with dynamin,<sup>9</sup> a protein essential for endocytosis. Particularly intriguing in the context of the SNc, PLD has also been shown to be stimulated by the  $D_2$  DA receptor, a G protein-coupled receptor and a key presynaptic regulator of DA homeostasis.<sup>37-40</sup> One possibility, therefore, is that PLD2 may be part of feedback loop that is necessary to downregulate the  $D_2$  receptor by endocytosis. However, any one of the known functions of PLD2 could be part of the mechanism that leads to loss of DA neurons when PLD2 is overexpressed and to increased DA signaling when it is knocked down. In this respect, we note again that we found significantly higher interaction of  $\alpha$ -syn and PLD2 in striatal (presumably synaptic) tissue rather than nigral tissue, in spite of the fact that the concentration of PLD2 appeared to be higher in nigral tissue (Figure 6).

Finally, this study raises the question why  $\alpha$ -syn knockouts show little pathology. The loss of  $\alpha$ -syn should increase PLD2 activity, yet little neurodegeneration is seen in  $\alpha$ -syn knockout mice.<sup>41,42</sup> A possible explanation is that rodent SNc is one of the few tissues

that robustly expresses all three synucleins ( $\alpha$ ,  $\beta$ , and  $\gamma$ ),<sup>41</sup> and knockout mice may be capable of altering expression of redundant synucleins during development. Indeed, all three of the synucleins are potent inhibitors of PLD2 *in vitro*.<sup>7</sup> To see whether siRNA knockdown of  $\alpha$ -syn produces the same neurodegeneration seen with overexpression of PLD2, we recently used gene transfer to express  $\alpha$ -syn siRNAs in rat SNc. In contrast to mouse knockouts, siRNA knockdown of  $\alpha$ -syn in adult rat SNc resulted in severe, acute SNc neurodegeneration with a time course similar to that seen here when PLD2 was overexpressed.<sup>43</sup>

Taken together, our data suggest that an important role for  $\alpha$ -syn may be to regulate PLD2 activity *in vivo*. Our data also clearly suggest that the level of PLD2 activity is critical for DA regulation. Finally, the data suggest that  $\alpha$ -syn toxicity in humans may be related, in part, to aberrant PLD2 regulation, and that PLD2 may be a target for Parkinson disease therapy.

### MATERIALS AND METHODS

**rAAV vectors.** All vectors have been packaged in AAV5 capsid and purified as described previously.<sup>5,14</sup> The *PLD2* gene was generated by PCR from rat mRNA using 5' sense primers corresponding to the start codon, with the addition of a Kozak sequence for optimal translation initiation. This sequence contains an NcoI site that was used to place the gene in frame with an N-terminal HA tag. An NsiI site was engineered in the 3' reverse primer after the stop codon. The PCR product was digested with these enzymes and cloned into NcoI-BglII digested pSOFFTR5 to produce the pSf5HAPLD vector, referred to here as the PLD2 rAAV vector. pSOFFTR5 is an rAAV5 vector plasmid containing AAV5 terminal repeats. Rat  $\alpha$ -syn cDNA and human wt  $\alpha$ -syn were cloned into rAAV as previously described for human wt  $\alpha$ -syn.<sup>5</sup> Myocardin siRNA virus was the kind gift of Al Lewin. Virus titers (vector genomes per ml) were determined by dot blot assay<sup>44,45</sup> and were for PLD2-HA:  $4.54 \times 10^{11}$ ; human  $\alpha$ -syn:  $8.87 \times 10^{12}$ ; PLD2 siRNA:  $3.44 \times 10^{12}$ ; rat  $\alpha$ -syn:  $2.9 \times 10^{12}$ ; myocardin siRNA:  $2.63 \times 10^{12}$ ; S129D:  $1.02 \times 10^{13}$ . When compared with RT-PCR assays, dot blot assays were typically eight- to tenfold higher than RT-PCR assays as performed in our laboratory.

**rAAV-shRNA plasmid construction.** shRNAs were designed based on accession number NM033299 for rat PLD2 and NM030992 for rat PLD1. All sequences were BLAST-confirmed for specificity. Synthetic DNA encoding shRNA targeting PLD2 was cloned into a U6 promoter-driven AAV vector developed in our laboratory. shRNA vector plasmids were then co-transfected with AAV vectors expressing target genes (2:1 ratio) or with empty vector as control into 293 cells for 48 hours for knockdown analyses of gene expression by immunoblotting. An shRNA plasmid that showed the greatest effects, about 90% knockdown efficiency (pTR2-rPLD siRNA2), was chosen for virus packaging as described above. The shRNA target sequence used for PLD2 was AAGCGCGACAGTGAGCTAG. The myocardin shRNA target was TGCAACTGCAGAAGCAGAA.

**Intracerebral injections.** All surgeries were performed as previously described.<sup>5</sup> The rats were placed in the stereotaxic frame, and rAAV vectors were injected into the SNc (AP -5.6 mm, LAT -2.4 mm from bregma and DV -7.2 mm from dura), through a glass micropipette with an inner diameter ~30-40  $\mu\text{m}$  at a rate of 0.5  $\mu\text{l}$  per minute. Animals were injected with a total of 1.5  $\mu\text{l}$  containing ~0.5-10  $\times 10^9$  vector genomes of the appropriate gene as determined by dot blot assay (and ~8-10 times lower when assayed by RT-PCR). The input titers were below those that have been seen to produce chronic inflammatory responses in some studies,<sup>17</sup> and no evidence of chronic inflammation was seen.

**Tissue preparation.** Animals were deeply anesthetized by pentobarbital injection. Brains were removed and divided into two parts at approximately

–3.5 mm behind bregma. The caudal part containing the SNc was fixed in the ice-cold 4% paraformaldehyde in 0.1 mol/l phosphate buffer, pH 7.4. The rostral piece of brain tissue was dissected on the right and left striatum. The tissue pieces were weighed, frozen separately on dry ice and kept at  $-80^{\circ}\text{C}$  until assayed. The fixed part of brains was stored overnight at  $4^{\circ}\text{C}$  and then transferred into 30% sucrose in 0.1 mol/l phosphate buffer for cryoprotection. Forty-micrometer thick coronal sections were cut on a freezing stage sliding microtome.

**Immunohistochemistry.** For bright-field microscopy analysis, sections were preincubated first with 1%  $\text{H}_2\text{O}_2$ –10% methanol for 15 minutes and then with 5% normal goat serum for 1 hour. Sections were incubated overnight at room temperature with mouse anti-TH (Chemicon, Temecula, CA, at 1:2,000 dilution) or mouse anti- $\alpha$ -syn (BD Laboratories, Franklin Lakes, NJ) antibodies. Incubation with biotinylated secondary antibody was followed by incubation with avidin–biotin–peroxidase complex (Vector Laboratories, Burlingame, CA). Reactions were visualized using 3,3'-diaminobenzidine (DAB).

For confocal microscopy, sections were incubated with the indicated primary antibodies for human  $\alpha$ -syn, TH, and HA (Abcam, Cambridge, MA), VMAT (Santa Cruz, Santa Cruz, CA) and a secondary antibody labeled with Cy2 or Cy5 (Jackson ImmunoResearch Laboratories, West Grove, PA). The sections were examined with a Leica laser scanning confocal microscope (Leica Microsystems CMS, Mannheim, Germany).

**Striatal DA measurements.** Three milligrams of starting tissue were thawed in 1 ml of 0.1 N  $\text{HClO}_4$  containing dihydroxybenzylamine as an internal control and homogenized. The sample was centrifuged and the supernatant was filtered through a 0.2  $\mu\text{m}$  filter. DA and DOPAC levels were analyzed on a Beckman Gold System (Beckman Coulter, Brea, CA) using a C18 Waters Symmetry column (Waters, Milford, MA) and an ESA Coulochem electrochemical detector (ESA, Chelmsford, MA) equipped with a 5011A analytical cell. The mobile phase was as follows: 8.2 mmol/l citric acid, 8.5 mmol/l sodium phosphate monobasic, 0.25 mmol/l EDTA, 0.30 mmol/l sodium octyl sulfate, and 7.0% acetonitrile, pH 3.5.

**Unbiased stereology.** The unbiased stereological estimation of the total number of the TH<sup>+</sup> neurons in SNc was performed as previously described.<sup>5</sup> Taking into account that some effects of the AAV vectors hypothetically might downregulate the TH phenotype and lead to a mistaken sense of cell loss, we evaluated the number of total neurons using additional series of brain sections stained with cresyl violet or with antibody to AADC.

**PLD2 RT-PCR.** Tissues were suspended in 300  $\mu\text{l}$  of lysis buffer (50 mmol/l Tris, pH 7.5, 0.15 mol/l NaCl) containing protease mixture and RNase inhibitor (Roche, Basel, Switzerland) and homogenized for 10 seconds. Total RNA was isolated from 100  $\mu\text{l}$  of lysate by using TRIzol (Invitrogen, Carlsbad, CA). After DNase I treatment, 500 ng of RNA was reverse-transcribed in 25  $\mu\text{l}$  reaction using SuperScript III first-strand cDNA synthesis kit (Invitrogen). Real-time PCR was performed on the MyiQ Single-Color Real-Time PCR Detection System (Bio-Rad, Hercules, CA) using IQ SYBR Green Supermix (Bio-Rad), 2  $\mu\text{l}$  of cDNA, and PLD2 primers. All values obtained were normalized with respect to levels of  $\beta$ -actin mRNA. The primer pairs used for RT-PCR experiments were forward 5'-CTGAACTCCAGCCAGTTGCA-3' and reverse 5'-CGCTGGTGTATCTTTCGGTG-3' for PLD2 gene, and forward 5'-CACTGCCGCATCTCTTCTCT-3' and reverse 5'-AACCGCTCATTGCCGATAGTG-3' for  $\beta$ -actin gene. The primer pairs used for PLD1 were forward 5'-GGAAGGCCAGAGATATCGAG-3' and reverse 5'-GCCTGTGGAAATGTCTCCTT-3'. All real-time PCRs were performed in duplicate using RNA from individual rats to give an average value for each animal. Serial dilutions of plasmid DNA containing PLD2 gene were used as standard templates. Relative quantification was performed using the  $\Delta\text{Ct}$  method.

**Immunoblotting.** Tissue homogenates described above were adjusted to a final concentration of 1% NP-40, 0.1% SDS, incubated on ice for 30 minutes and centrifuged for 15 minutes at  $4^{\circ}\text{C}$ . Protein concentrations were determined by Bradford. Fifty micrograms of each lysate were separated on Bio-Rad precast 4–20% SDS-PAGE gradient gel, transferred to PVDF (Millipore, Billerica, MA) membranes and immunoblotted. Membranes were incubated with primary antibodies for 2 hours at RT or  $4^{\circ}\text{C}$  overnight. Primary antibodies were diluted at a 1:1,000 anti-PLD2 antibody (Abcam), 1:2,000 human  $\alpha$ -syn antibody (BD, Franklin Lakes, NJ), 1:2,000 rat + human  $\alpha$ -syn antibody (Invitrogen), 1:2,000 anti-TH (Chemicon), or 1:5,000 GAPDH antibody (Abcam) prior to incubation. After washing, membranes were incubated with peroxidase-conjugated secondary antibody for 1 hour. Peroxidase-conjugated HA (Roche) antibody was used to detect HA-tagged proteins. Western blots were washed, developed with Immobilon-Western (Millipore) and exposed to films.

**Rotational behavior.** Drug-induced rotational behavior was measured following an injection of D-amphetamine sulfate (2.5 mg/kg i.p.; Sigma, St Louis, MO) at 4, 8, and 26 weeks after the viral injection. Rotations were measured during a 90-minute period, and full  $360^{\circ}$  turns were counted.

**Statistical analysis.** Data were analyzed using one tailed unpaired *t*-test, one-way analysis of variance with Tukey post-test, or two-way analysis of variance with Bonferroni post-test using Prism 4 (GraphPad Software, La Jolla, CA).

## SUPPLEMENTARY MATERIAL

**Figure S1.** Effect of PLD2, PLD2 siRNA, and  $\alpha$ -syn on striatal DA.

**Figure S2.** Effect of PLD2 and  $\alpha$ -syn on amphetamine induced rotation.

**Figure S3.** PLD2 siRNA suppresses PLD2 mRNA and protein expression *in vivo*.

**Figure S4.** Unbiased estimation of TH<sup>+</sup> cells remaining in SNc after expression of  $\alpha$ -syn, PLD2 siRNA or both.

**Figure S5.** Amphetamine induced rotation of PLD2 siRNA injected animals at 8 weeks post injection.

## ACKNOWLEDGMENTS

This work was supported by a program project grant (to N.M.) from the National Institutes of Health (PO1 NS36302) and by the ACS Koger endowment to N.M. N.M. is an inventor of patents related to recombinant AAV technology and owns equity in a gene therapy company that is commercializing AAV for gene therapy applications. We thank Joyce Feller, Jacques Tessier, and Isabelle Williams for their able technical assistance.

## REFERENCES

1. Cookson, MR and van der Brug, M (2008). Cell systems and the toxic mechanism(s) of alpha-synuclein. *Exp Neurol* **209**: 5–11.
2. Jenco, JM, Rawlingson, A, Daniels, B and Morris, AJ (1998). Regulation of phospholipase D2: selective inhibition of mammalian phospholipase D isoenzymes by alpha- and beta-synucleins. *Biochemistry* **37**: 4901–4909.
3. Jenkins, GM and Frohman, MA (2005). Phospholipase D: a lipid centric review. *Cell Mol Life Sci* **62**: 2305–2316.
4. Ahn, BH, Rhim, H, Kim, SY, Sung, YM, Lee, MY, Choi, JY *et al.* (2002). alpha-Synuclein interacts with phospholipase D isozymes and inhibits pervanadate-induced phospholipase D activation in human embryonic kidney-293 cells. *J Biol Chem* **277**: 12334–12342.
5. Gorbatyuk, OS, Li, S, Sullivan, LF, Chen, W, Kondrikova, G, Manfredsson, FP *et al.* (2008). The phosphorylation state of Ser-129 in human alpha-synuclein determines neurodegeneration in a rat model of Parkinson disease. *Proc Natl Acad Sci USA* **105**: 763–768.
6. Azeredo da Silveira, S, Schneider, BL, Cifuentes-Diaz, C, Sage, D, Abbas-Terki, T, Iwatsubo, T *et al.* (2009). Phosphorylation does not prompt, nor prevent, the formation of alpha-synuclein toxic species in a rat model of Parkinson's disease. *Hum Mol Gen* **18**: 872–887.
7. Payton, JE, Perrin, RJ, Woods, WS and George, JM (2004). Structural determinants of PLD2 inhibition by alpha-synuclein. *J Mol Biol* **337**: 1001–1009.
8. Oude Weernink, PA, López de Jesús, M and Schmidt, M (2007). Phospholipase D signaling: orchestration by PIP2 and small GTPases. *Naunyn Schmiedebergs Arch Pharmacol* **374**: 399–411.

9. Di Fulvio, M, Frondorf, K, Henkels, KM, Lehman, N and Gomez-Cambronero, J (2007). The Grb2/PLD2 interaction is essential for lipase activity, intracellular localization and signaling in response to EGF. *J Mol Biol* **367**: 814–824.
10. Zhao, C, Du, G, Skowronek, K, Frohman, MA and Bar-Sagi, D (2007). Phospholipase D2-generated phosphatidic acid couples EGFR stimulation to Ras activation by Sos. *Nat Cell Biol* **9**: 706–712.
11. Iwata, A, Miura, S, Kanazawa, I, Sawada, M and Nukina, N (2001). alpha-Synuclein forms a complex with transcription factor Elk-1. *J Neurochem* **77**: 239–252.
12. Cazzoli, R, Shemon, AN, Fang, MQ and Hughes, WE (2006). Phospholipid signalling through phospholipase D and phosphatidic acid. *IUBMB Life* **58**: 457–461.
13. Lee, CS, Kim, IS, Park, JB, Lee, MN, Lee, HY, Suh, PG *et al.* (2006). The phox homology domain of phospholipase D activates dynamin GTPase activity and accelerates EGFR endocytosis. *Nat Cell Biol* **8**: 477–484.
14. Burger, C, Gorbatyuk, OS, Velardo, MJ, Peden, CS, Williams, P, Zolotukhin, S *et al.* (2004). Recombinant AAV viral vectors pseudotyped with viral capsids from serotypes 1, 2, and 5 display differential efficiency and cell tropism after delivery to different regions of the central nervous system. *Mol Ther* **10**: 302–317.
15. McFarland, NR, Lee, JS, Hyman, BT and McLean, PJ (2009). Comparison of transduction efficiency of recombinant AAV serotypes 1, 2, 5, and 8 in the rat nigrostriatal system. *J Neurochem* **109**: 838–845.
16. Paterna, JC, Feldon, J and Büeler, H (2004). Transduction profiles of recombinant adeno-associated virus vectors derived from serotypes 2 and 5 in the nigrostriatal system of rats. *J Virol* **78**: 6808–6817.
17. Ulusoy, A, Sahin, G, Björklund, T, Aebischer, P and Kirik, D (2009). Dose optimization for long-term rAAV-mediated RNA interference in the nigrostriatal projection neurons. *Mol Ther* **17**: 1574–1584.
18. Peden, CS, Manfredsson, FP, Reimsnider, SK, Poirier, AE, Burger, C, Muzyczka, N *et al.* (2009). Striatal readministration of rAAV vectors reveals an immune response against AAV2 capsids that can be circumvented. *Mol Ther* **17**: 524–537.
19. Reimsnider, S, Manfredsson, FP, Muzyczka, N and Mandel, RJ (2007). Time course of transgene expression after intrastriatal pseudotyped rAAV2/1, rAAV2/2, rAAV2/5, and rAAV2/8 transduction in the rat. *Mol Ther* **15**: 1504–1511.
20. Peng, X, Peng, XM, Tehrani, R, Dietrich, P, Stefanis, L and Perez, RG (2005). Alpha-synuclein activation of protein phosphatase 2A reduces tyrosine hydroxylase phosphorylation in dopaminergic cells. *J Cell Sci* **118**(Pt 15): 3523–3530.
21. Mandel, RJ, Spratt, SK, Snyder, RO and Leff, SE (1997). Midbrain injection of recombinant adeno-associated virus encoding rat glial cell line-derived neurotrophic factor protects nigral neurons in a progressive 6-hydroxydopamine-induced degeneration model of Parkinson's disease in rats. *Proc Natl Acad Sci USA* **94**: 14083–14088.
22. Moore, AE, Cicchetti, F, Hennen, J and Isacson, O (2001). Parkinsonian motor deficits are reflected by proportional A9/A10 dopamine neuron degeneration in the rat. *Exp Neurol* **172**: 363–376.
23. Du, G, Huang, P, Liang, BT and Frohman, MA (2004). Phospholipase D2 localizes to the plasma membrane and regulates angiotensin II receptor endocytosis. *Mol Biol Cell* **15**: 1024–1030.
24. Kirik, D, Rosenblad, C, Burger, C, Lundberg, C, Johansen, TE, Muzyczka, N *et al.* (2002). Parkinson-like neurodegeneration induced by targeted overexpression of alpha-synuclein in the nigrostriatal system. *J Neurosci* **22**: 2780–2791.
25. Grimm, D, Streetz, KL, Jopling, CL, Storm, TA, Pandey, K, Davis, CR *et al.* (2006). Fatality in mice due to oversaturation of cellular microRNA/short hairpin RNA pathways. *Nature* **441**: 537–541.
26. McBride, JL, Boudreau, RL, Harper, SQ, Staber, PD, Montey, AM, Martins, I *et al.* (2008). Artificial miRNAs mitigate shRNA-mediated toxicity in the brain: implications for the therapeutic development of RNAi. *Proc Natl Acad Sci USA* **105**: 5868–5873.
27. Lo Bianco, C, Ridet, JL, Schneider, BL, Deglon, N and Aebischer, P (2002). alpha-Synucleinopathy and selective dopaminergic neuron loss in a rat lentiviral-based model of Parkinson's disease. *Proc Natl Acad Sci USA* **99**: 10813–10818.
28. Chandra, S, Gallardo, G, Fernández-Chacón, R, Schlüter, OM and Südhof, TC (2005). Alpha-synuclein cooperates with CSPalpha in preventing neurodegeneration. *Cell* **123**: 383–396.
29. Wakamatsu, M, Ishii, A, Ukai, Y, Sakagami, J, Iwata, S, Ono, M *et al.* (2007). Accumulation of phosphorylated alpha-synuclein in dopaminergic neurons of transgenic mice that express human alpha-synuclein. *J Neurosci Res* **85**: 1819–1825.
30. Rappley, I, Gitler, AD, Selvy, PE, LaVoie, MJ, Levy, BD, Brown, HA *et al.* (2009). Evidence that alpha-synuclein does not inhibit phospholipase D. *Biochemistry* **48**: 1077–1083.
31. Klein, J (2005). Functions and pathophysiological roles of phospholipase D in the brain. *J Neurochem* **94**: 1473–1487.
32. Sciorra, VA, Rudge, SA, Prestwich, GD, Frohman, MA, Engebrecht, J and Morris, AJ (1999). Identification of a phosphoinositide binding motif that mediates activation of mammalian and yeast phospholipase D isoenzymes. *EMBO J* **18**: 5911–5921.
33. Singer, WD, Brown, HA, Jiang, X and Sternweis, PC (1996). Regulation of phospholipase D by protein kinase C is synergistic with ADP-ribosylation factor and independent of protein kinase activity. *J Biol Chem* **271**: 4504–4510.
34. Bhattacharya, M, Babwah, AV, Godin, C, Anborgh, PH, Dale, LB, Poulter, MO *et al.* (2004). Ral and phospholipase D2-dependent pathway for constitutive metabotropic glutamate receptor endocytosis. *J Neurosci* **24**: 8752–8761.
35. Dhami, GK and Ferguson, SS (2006). Regulation of metabotropic glutamate receptor signaling, desensitization and endocytosis. *Pharmacol Ther* **111**: 260–271.
36. Oude Weernink, PA, Han, L, Jakobs, KH and Schmidt, M (2007). Dynamic phospholipid signaling by G protein-coupled receptors. *Biochim Biophys Acta* **1768**: 888–900.
37. Everett, PB and Senogles, SE (2004). D3 dopamine receptor activates phospholipase D through a pertussis toxin-insensitive pathway. *Neurosci Lett* **371**: 34–39.
38. Senogles, SE (2000). The D2s dopamine receptor stimulates phospholipase D activity: a novel signaling pathway for dopamine. *Mol Pharmacol* **58**: 455–462.
39. Senogles, SE (2003). D2s dopamine receptor mediates phospholipase D and antiproliferation. *Mol Cell Endocrinol* **209**: 61–69.
40. Senogles, SE (2007). D2 dopamine receptor-mediated antiproliferation in a small cell lung cancer cell line, NCI-H69. *Anticancer Drugs* **18**: 801–807.
41. Abeliovich, A, Schmitz, Y, Fariñas, I, Choi-Lundberg, D, Ho, WH, Castillo, PE *et al.* (2000). Mice lacking alpha-synuclein display functional deficits in the nigrostriatal dopamine system. *Neuron* **25**: 239–252.
42. Cabin, DE, Shimazu, K, Murphy, D, Cole, NB, Gottschalk, W, McIlwain, KL *et al.* (2002). Synaptic vesicle depletion correlates with attenuated synaptic responses to prolonged repetitive stimulation in mice lacking alpha-synuclein. *J Neurosci* **22**: 8797–8807.
43. Gorbatyuk, OS, Li, S, Nash, K, Gorbatyuk, M, Lewin, AS, Sullivan, LF *et al.* (2010). *In vivo* RNAi-mediated alpha-synuclein silencing induces nigrostriatal degeneration. *Mol Ther* (epub ahead of print).
44. Zolotukhin, S, Byrne, BJ, Mason, E, Zolotukhin, I, Potter, M, Chesnut, K *et al.* (1999). Recombinant adeno-associated virus purification using novel methods improves infectious titer and yield. *Gene Ther* **6**: 973–985.
45. Zolotukhin, S, Potter, M, Zolotukhin, I, Sakai, Y, Loiler, S, Frait, TJ Jr *et al.* (2002). Production and purification of serotype 1, 2, and 5 recombinant adeno-associated viral vectors. *Methods* **28**: 158–167.